Materials Research Bulletin 47 (2012) 2380–2388

Contents lists available at SciVerse ScienceDirect

Materials Research Bulletin

journal homepage: www.elsevier.com/locate/matresbu

Converting environmentally hazardous materials into clean energy using a novel nanostructured photoelectrochemical fuel cell

Yong X. Gan [a,*], Bo J. Gan [b], Evan Clark [a], Lusheng Su [a], Lihua Zhang [c]

[a] Department of Mechanical, Industrial and Manufacturing Engineering, College of Engineering, University of Toledo, Toledo, OH 43606, USA
[b] Ottawa Hills High School, 2532 Evergreen Road, Toledo, OH 43606, USA
[c] Center for Functional Nanomaterials, Brookhaven National Laboratory, Upton, NY 11973, USA

ARTICLE INFO

Article history:
Received 24 November 2011
Received in revised form 25 March 2012
Accepted 21 May 2012
Available online 4 June 2012

Keywords:
A. Nanostructures
C. Electron microscopy
D. Catalytic properties
D. Electrochemical properties
D. Microstructure

ABSTRACT

In this work, a novel photoelectrochemical fuel cell consisting of a titanium dioxide nanotube array photosensitive anode and a platinum cathode was made for decomposing environmentally hazardous materials to produce electricity and clean fuel. Titanium dioxide nanotubes (TiO_2 NTs) were prepared via electrochemical oxidation of pure Ti in an ammonium fluoride and glycerol-containing solution. Scanning electron microscopy was used to analyze the morphology of the nanotubes. The average diameter, wall thickness and length of the as-prepared TiO_2 NTs were determined. The photosensitive anode made from the highly ordered TiO_2 NTs has good photo-catalytic property, as proven by the decomposition tests on urea, ammonia, sodium sulfide and automobile engine coolant under ultraviolet (UV) radiation. To improve the efficiency of the fuel cell, doping the TiO_2 NTs with a transition metal oxide, NiO, was performed and the photosensitivity of the doped anode was tested under visible light irradiation. It is found that the NiO-doped anode is sensitive to visible light. Also found is that polyaniline-doped photosensitive anode can harvest photon energy in the visible light spectrum range much more efficiently than the NiO-doped one. It is concluded that the nanostructured photoelectrochemical fuel cell can generate electricity and clean fuel by decomposing hazardous materials under sunlight.

1. Introduction

Energy sustainability and environmental sustainability are the two global issues. What are the solutions to these issues? How the future sustainability of the world can be built? During the last 20 years, the global energy need drove new technology advancement. For example, solar energy conversion [1–3] has achieved great success. Waste recycling [4,5], hydrogen production [6–9], biofuel conversion [10] have also been studied as alternatives for energy generation. Specifically, photoelectrochemical fuel cells running by harvesting solar energy have recently been explored [11]. Photocatalysis has been demonstrated successful for the clean fuel, e.g. hydrogen production [12]. The photochemical fuel cell approach has been considered as a relatively simple and inexpensive way to harvest solar energy for clean fuel production. The ability of generating energy from solid waste and/or wastewater under the irradiation of sunlight, while cleaning the environment and producing water for reuse has caught a lot of interests. Energy conversion and environment cleaning become strong incentives to develop this technology [13–15].

It must be noted that using photochemical fuel cells for clean energy production has been proposed for a considerably long time [16–22]. However, many problems still remain to be solved. For example, the efficiency of hydrogen production from photocatalytic reactions is very low [21]. The problem comes from the poor performance of the photosensitive anode. Recently, many researchers have made significant effort on searching new anode materials. Titanium oxide particles were found to have relatively high quantum efficiency and hydrogen generation rate [23–25]. It has been shown that such particulate materials can decompose organic substances to generate electricity and hydrogen simultaneously under ultraviolet (UV) and visible irradiations [26].

Nanomaterials, for example nanoparticles, have much higher surface areas than their bulk counterparts so that more intensive photocatalytic reactions occur at the surface of the nanoparticels [27,28]. TiO_2 nanoparticles have the potential for clean fuel and electricity generation by decomposing waste materials [29]. Nevertheless, the agglomeration of particles is a challenging problem to be solved in order to keep the high surface area for different applications [30,31]. Two ways have been proposed to potentially solve the agglomeration problem [32,33]. The first way

---

* Corresponding author. Tel.: +1 419 530 6007; fax: +1 419 530 8206.
E-mail address: yong.gan@utoledo.edu (Y.X. Gan).

0025-5408/$ – see front matter © 2012 Elsevier Ltd. All rights reserved.
http://dx.doi.org/10.1016/j.materresbull.2012.05.049

is to control the material growth along certain preferential directions to form nanoscale fractals or dendrites, which prevents the agglomeration of nanoparticles on substrates [32]. The other method is to use nanoporous templates because confined growth of nanocrystals either within the nanopores or at the surface of the templates can be established to prevent nanoparticle agglomeration [33].

Clean energy generation from hazardous materials is a fascinating research topic. For example, hydrogen generation from ammonia was studied by Yin et al. using nanostructured catalysts [34]. The active components used include Ru, Rh, Pt, Pd, Ni, Fe. These components are supported by carbon nanotubes (CNTs) and other materials such as Al_2O_3, MgO, and ZrO_2. It has been found that CO-free hydrogen can be generated on these catalysts through ammonia decomposition. The CNT-supported catalyst showed the highest efficiency. TiO_2 was found very effective as the catalyst support for ammonia decomposition [34,35]. Since TiO_2 is photosensitive, decomposing organics at its surface has caught a lot of attentions. For example, it has found applications in decomposing spilled-oil for environmental cleaning, as reposted by Hsu et al. [36].

In this paper, we will present the work on using self-organized anodic titanium dioxide nanotube arrays to make a novel photoelectrochemical fuel cell anode with high surface area and strong photosensitivity. It will be demonstrated that under UV radiation, the solutions containing both organic and inorganic hazardous materials decompose at the titanium dioxide nanotube photosensitive anode. Urea, ammonia, sodium sulfide and automobile engine coolant are the waste materials for the photosensitive decomposing tests. These materials are environmentally hazardous. For example, the nitrogen-rich urea and ammonia promote algae growth in open water of the Great Lakers. Sulfide is a major pollutant substance generated from those power plants burning fossil fuels. The antifreeze/coolant contains ethylene glycol, which is poisonous for many biological species. When a low-hydrogen overpotential metal, Pt, is used as the cathode to form a photoelectrochemical fuel cell, hydrogen production at the Pt cathode is observed in this work. Preliminary research results of the open circuit voltage of the photoelectrochemical fuel cell and the dynamic response of the photosensitive anode to UV and visible light will be given.

2. Materials and experimental methods

2.1. Materials and instruments

Pure titanium (Ti) sheet ordered from McMaster.com with a thickness of 0.1 mm was used as the start material for making the self-organized TiO_2 nanotube (NT) arrays. Ammonia, urea, ammonium fluoride, sodium sulfide, and glycerol were purchased from Alfa Aesar. A solution containing 1.5 wt% NH_4F + 90 wt% glycerol and rest de-ionized (DI) water was made and used as the electrolyte for the electrochemical oxidation of the titanium sheet to generate nanotube arrays. Previous studies show that several types of organic or inorganic electrolytes may be used to make titanium oxide nanostructures. For example, Mackay et al. found that neutral NaF solutions can thicker the wall of the TiO_2 nanotubes [37] and Narayanan et al. showed that TiO_2 networks can be obtained in the Na_2SO_4 + NaF electrolyte [38]. Titanium oxide dissolves more uniformly in near-neutral or weak base solutions than in acids. The more uniform dissolution process helps the titanium oxide to self-organize into more regular nanotubes. That is why we have used the NH_4F and glycerol solution, which is a near neutral electrolyte. The power supply for the electrochemical oxidation of the titanium is a regulated DC power source, model HY5003 (0–50 V, 0–3 A). A Quanta 3D field emission scanning electron microscope (FESEM) was used for the nanotube morphology observation. The JEOL 2100F transmission electron microscope (TEM) was also used to observe the nanotubes and to generate high resolution TEM images. The ultraviolet lamp, UVL-21 (365 nm UV, 4 W, 0.16 A), was used to generate UV light and a 250 W electric bulb was used to generate visible light for photoelectrochemical decomposition experiments. The irradiation power on the photoelectrochemical fuel cell anode was about 40 mW/cm^2. A CHI 400 A electrochemical workstation was used to monitor the waste material decomposition process by measuring the open circuit voltage of the fuel cell. A tubular carbon dioxide sensor was connected to an Xplorer GLX data acquisition unit to measure the concentration of carbon dioxide associated with the decomposition of urea in the photoelectrochemical fuel cell.

Various aqueous solutions containing environmentally hazardous materials were made to perform photoelectrochemical decomposition tests using the nanostructured fuel cell anode. The justifications for choosing those hazardous materials for the studies are given as follows. Ammonia and urea are major compositions from fertilizers. They are pollutants in surface water. Diluted ammonia ($NH_3{\cdot}H_2O$) solutions were made with the concentration of 1 wt% (pH 10.63), 0.25 wt%, and 0.025 wt%. The concentrations for urea were 1.0 M, 0.5 M, and 0.25 M. Sulfide is the major composition from the burning of coal. It is harmful for environment. Although the directly released sulfides from coal burning have multiple constituents, we use sodium sulfide in the test for the preliminary study. The typical concentration of sodium sulfide solution used in this work is 0.5 M. The antifreeze/coolant with the brand name of PEAK® was purchased from WalMart. The reason for choosing an antifreeze/coolant for study is that automobile radiator flushing generates a lot of diluted coolant solution. The major composition for the antifreeze and cooling function in the original product is ethylene glycol, which is poisonous. According to the purchased product specification for this work, the concentration of ethylene glycol in the antifreeze/coolant is about 20 wt%.

2.2. TiO_2 nanotube anode and photochemical fuel cell fabrication

The 0.1 mm thick titanium (Ti) thin sheet with the size of 250 mm × 250 mm was cut into 40 mm × 5 mm × 0.1 mm samples. Self-organized TiO_2 NTs were prepared by electrochemical oxidation of the Ti samples in the electrolyte with 1.5% NH_4F + 90% glycerol + 8.5% water in weight. A two-electrode cell was used for the electrochemical oxidation of Ti at a room temperature of 25 °C. The anode and the cathode are the Ti samples with the same size. The distance between the two electrodes was 20 mm. The operation voltage was 50.0 V and the electrochemical oxidation time was 6 h. After electrochemical oxidation, the samples were rinsed in de-ionized water and air dried. The surface of the anode was completely covered by TiO_2 nanotube arrays as revealed by the electron microscopic analysis. After the TiO_2 NTs were prepared, high temperature annealing at 500 °C for 2 h was performed to crystallize the TiO_2. Then, the specimens were cooled down naturally, and they were used to make the photosensitive anode of the photoelectrochemical fuel cell. The photoelectrochemical fuel cell (PEFC) was in a one-compartment configuration as schematically shown in Fig. 1. The anode was made from the TiO_2 nanotube arrays set on the Ti. The cathode was Pt. The reference electrode used was Ag/AgCl. The main reaction at the cathode was hydrogen generation. Photoelectrochemical reactions happened at the anode and in the solutions to decompose the waste materials and generate electrons. Specifically, in the case of using urea solution, carbon dioxide was formed in the anode region. Electricity was also generated at the same time as measured by the CHI400A electrochemical workstation.

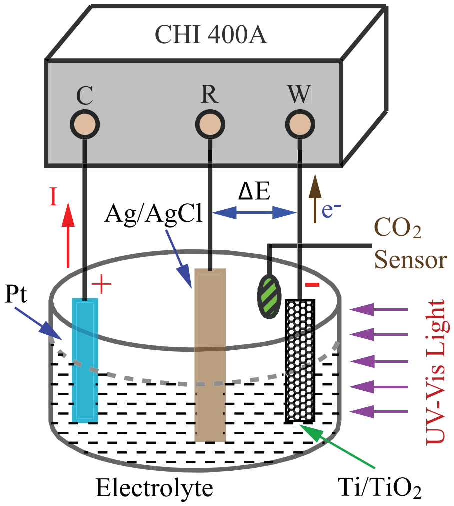

Fig. 1. Photoelectrochemical fuel cell with a TiO_2 nanotube anode and a Pt cathode.

3. Results and discussion

3.1. Surface morphology of the TiO_2 nanotube photoanode

Fig. 2 shows the schematic and the surface morphology of the anode with TiO_2 nanotube arrays. Fig. 2(a) sketches the TiO_2 nanotubes at the Ti sheet. Fig. 2(b) is a low magnification scanning electron microscopic (SEM) image, from which both the Ti substrate surface and the nanotubes can be seen. At higher magnification, the open end of the nanotubes is shown in Fig. 2(c). From the cross section view, separated nanotube bundles can be found in Fig. 2(d). It can be measured from Fig. 2(c) that the TiO_2 nanotubes have a diameter of about 150 nm. The wall thickness is about 20–30 nm. The cross-section view of the TiO_2 nanotubes (NTs) as shown in Fig. 2(d) reveals that the length of the nanotubes is about 1.5 μm. The increase in the concentration of NH_4F could result in deeper penetration of more F^- into the Ti substrate. Thus, the length of the NTs can be increased significantly.

If the electrochemical oxidation parameters such as the applied DC voltage and processing time were changed, the size of the TiO_2 NTs can also be changed, which was reported by other researchers using different electrolytes consisting of either HF or NH_4F [39,40]. Energy dispersive X-ray spectrum was also obtained (not shown here) using the same Quanta 3D field emission scanning electron microscope (FESEM). The analyzed region is 10 μm × 10 μm. The result shows that Ti and O are the major elements at the anode. Quantitative analysis gives the atomic ratio of Ti:O = 1:2, which means that the nanotubes have the stoichiometric composition of titanium dioxide. The weight percentage of each element is also calculated and reveals that the weight ratio of Ti:O equals to 3:2.

3.2. Growth mechanism of TiO_2 nanotube arrays

The formation of the titanium dioxide nanotubes in the electrolyte containing fluorine ions is the breakage of the passivation film or the pitting of the oxide film under the attack of the fluorine ions. Ti metal as the anode was oxidized first and the oxide film was dissolved into the electrolyte when the proper electrochemical conditions were established. The electrochemical

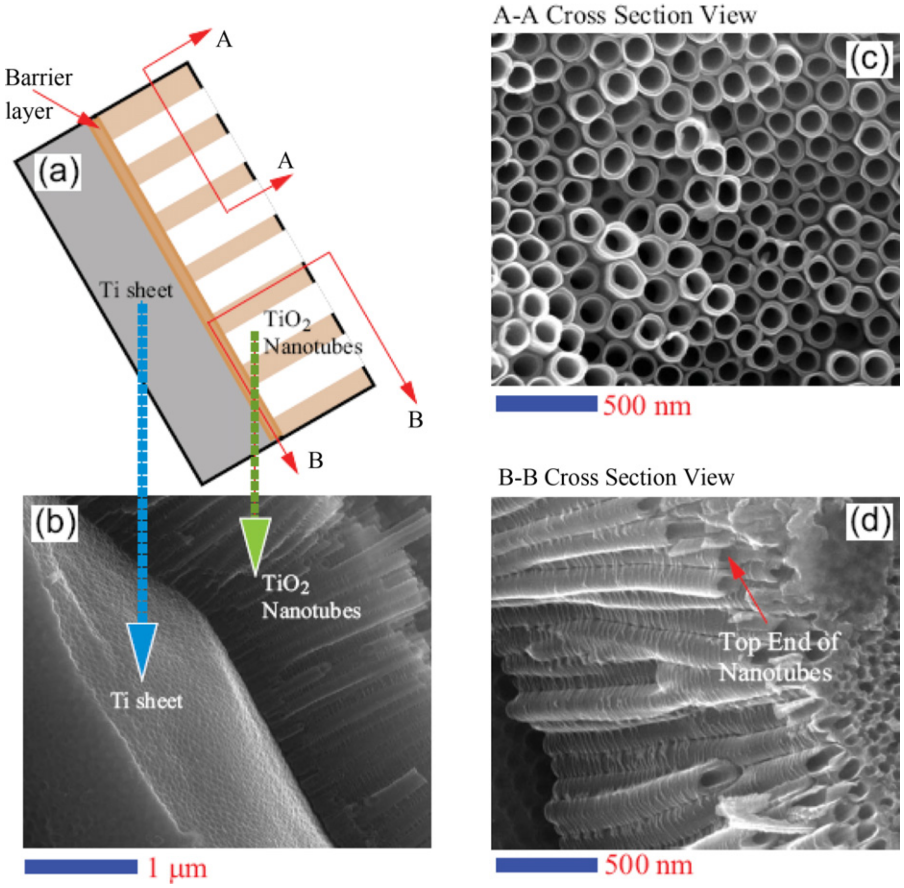

Fig. 2. Sketch and the surface morphology of the TiO_2 nanotube anode: (a) schematic of the photosensitive anode, (b) SEM image showing both the Ti substrate and the nanotube array, (c) SEM image showing the surface of the anode covered by self-organized nanotubes, (d) SEM image showing the cross-section of the nanotube array.

reactions related to the growth of the TiO_2 nanotube arrays have been studied and described as follows [41,42]:

$$\text{Hydrolyzation}: \quad 2H_2O \rightarrow O_2\uparrow + 4e^- + 4H^+ \tag{1}$$

$$\text{Cathode reaction}: \quad 2H^+ + 2e^- \rightarrow H_2\uparrow \tag{2}$$

$$\text{Film growth at anode}: \quad Ti + O_2 \rightarrow TiO_2 \tag{3}$$

$$\text{Film dissolution, nanotube growth}: \quad TiO_2 + 6F^- + 4H^+ \rightarrow [TiF_6]^{2-} + 2H_2O \tag{4}$$

In the electrochemical oxidation experiments, we used the electrolyte containing NH_4F and glycerol, which is almost a neutral solution. The hydrolyzation reaction of Eq. (1) helps to increase the acidity of the solution near the anode and provide oxygen for the oxide film formation. The reactions as described by Eqs. (2)–(4) explain why the TiO_2 nanotube arrays can grow on the surface of Ti anode and the hydrogen gas gives off at the cathode, even though both electrodes are the same Ti sheet samples.

Investigating the size distribution of the prepared TiO_2 nanotubes is meaningful for further understanding the formation mechanisms of the nanotubes. The results are also helpful for identifying proper electrochemical processing parameters, especially the electrolyte concentration effect. In addition, the size distribution can provide the basis for measuring the effective surface area of the photocatalytic anode in the photoelectrochemical fuel cell. Therefore, more statistic analyses based on diameter and length measurements of the NTs using multiple SEM images taken from various samples may be necessary. But this is not the focus of the current work. We leave it for future studies.

Electrochemical processing parameters, for example, the peak voltage used for processing the nanotubes, have significant impact on the geometry of the tubes. It is commonly known that the higher the voltage applied to a dielectric material, the deeper the material will be affected. Therefore, if a high voltage is applied, the length of the nanotubes increases. Narayanan et al. found that the voltage change results in the morphology evolution from flat structures to nanotubular networks [38]. How the applied voltage affects the radial size of the nanotubes is an interesting topic. It is found that the higher the voltage applied, the thicker the wall of the nanotubes. What the exact reason is still remains to be studied.

3.3. *Photocatalytic property of the of TiO_2 nanotube anode*

The four fluids containing hazardous materials were inducted into the one-compartment photoelectrochemical fuel cell. UV radiation was generated by the light source as shown in Fig. 1. Indeed, only the anode is necessary to be kept under the irradiation. It is observed that there is a voltage across the two electrodes of the fuel cell. At the Pt cathode, hydrogen bubbles formed in ammonia and the coolant solutions as long as the fuel cell is air-tight and the UV lamp is on. The open circuit voltage was measured as a function of time using the CHI400A electrochemical workstation. Also recorded are the dynamic response data when the UV light ON and OFF were switched. Fig. 3(a) and (b) show the open circuit potential (ΔE) vs. time (t) curves obtained from the tests on the solutions containing 1.0 M urea and 1% ammonia, respectively. Both Fig. 3(a) and (b) show that when the UV light is ON, the voltage at the photosensitive anode drops to −0.33 V within 150 s. When the UV light is OFF, the voltage goes up.

When the UV light is ON (i.e. in the charging cycle), the change in the anode potential as a function of irradiation time, t, may be expressed as:

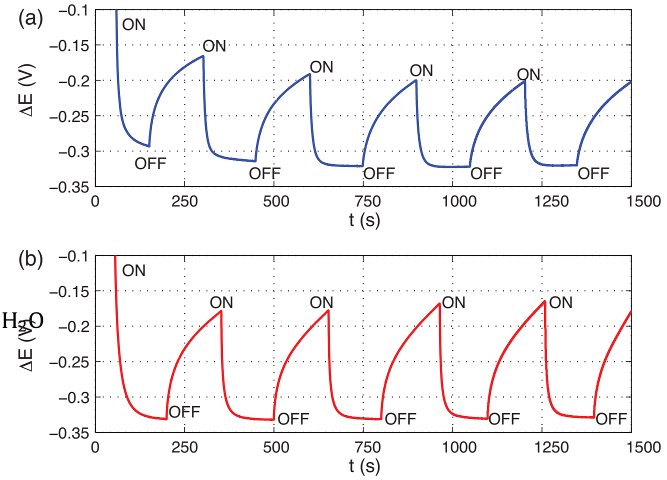

Fig. 3. Open circuit voltage and dynamic response of the photoelectrochemical fuel cell: (a) potential (ΔE) vs. time (t) from the test on the solution containing 1.0 M urea, (b) potential (ΔE) vs. time (t) from the test on the solution containing 1% ammonia.

$$\Delta E = Ae^{-Bt} - E_o$$

where A and B are constants associated with the charging cycle, and E_o is the equilibrium potential. When the UV light is OFF (i.e. in the discharging cycle), the change in the potential is a function of recovery or relaxation time, t, which is in the form as follows:

$$\Delta E = E_o - Ce^{-Dt}$$

where C and D are constants related to the discharging cycle.

In the urea solution, the main photosensitive reaction at the anode is as follows:

$$TiO_2 + h\nu\,(\text{UV light}) \rightarrow TiO_2(h^+) + TiO_2(e^-) \tag{5}$$

where h^+ and e^- stand for hole and electron, respectively. In the solution, urea decomposes by combination with the holes.

$$O{=}C(NH_2)_2 + 6h^+ + H_2O \rightarrow CO_2\uparrow + N_2\uparrow + 6H^+ \tag{6}$$

At the cathode, clean water generation is the main reaction.

$$O_2 + 4e^- + 4H^+ \rightarrow 2H_2O \tag{7}$$

If the cathode region is sealed or oxygen-free, hydrogen generation, i.e. Eq. (2), becomes the main reaction. The measurement results clearly reveal that the photodecomposition of urea and ammonia solutions can generate electricity. In addition, the clean fuel, hydrogen, can be produced when the cell was air-tight or oxygen-free.

In the ammonia solution, the main reaction at the anode is still the electron–hole charge pair generation under the excitation of photons. Nitrogen gas forms in the solution due to the combination of hole with ammonia, i.e.

$$2NH_3 + 6h^+ + H_2O \rightarrow N_2\uparrow + 6H^+ \tag{8}$$

While at the cathode, either hydrogen or clean water generation is the main reaction depending on the availability of oxygen.

To verify the carbon dioxide formation in the anodic region, data generated by the CO_2 gas sensor as shown in Fig. 1 were plotted. The plots are illustrated in Fig. 4. From the results shown in this figure, when the UV light was OFF, the concentration of CO_2 gas in the anode region of the fuel cell was less then 700 ppm. After the UV light was ON for about 5 min and the fuel cell was running in

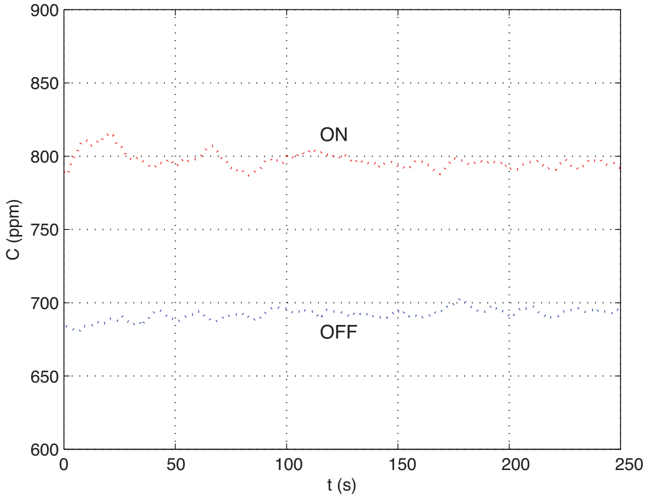

Fig. 4. Carbon dioxide concentration, ΔC, vs. time, t measured in the anode region of the fuel cell.

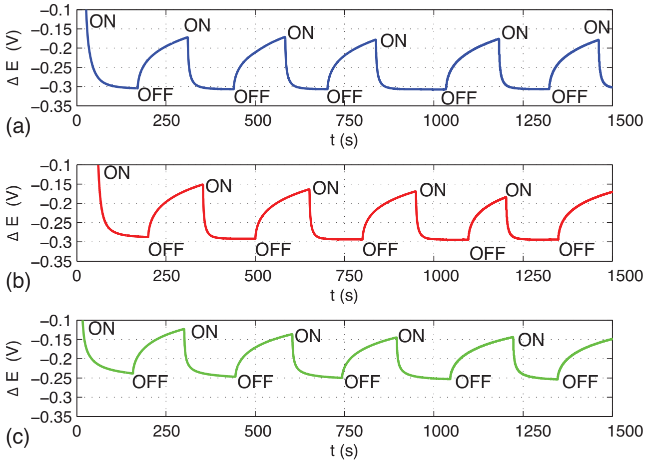

Fig. 6. Effect of concentration on the open circuit voltage of the fuel cell use ammonia as the fuel: (a) 0.5% ammonia, (b) 0.25% ammonia, (c) 0.025% ammonia.

the steady state, detectable CO_2 gas was generated. The monitored CO_2 gas concentration increased to 800 ppm. This confirms the reaction of Eq. (6) at the anode or in the region near the anode.

Comparative studies of the photocatalytic behavior of the TiO_2 nanotube anode in the urea solutions with different concentrations were performed. The urea solutions used have the concentrations of 0.5 M and 0.25 M. An obvious concentration effect was identified as shown by the results in Fig. 5. When the urea solution with the concentration of 0.5 M was used, the potential changed from 0.05 V to −0.2 V when the UV light was ON. Fig. 5(a) shows the dynamic response of potential, ΔE, vs. time, t, for TiO_2 nanotube anode to UV light in the 0.5 M urea solution. For the 0.25 M urea solution, smaller changes in the voltage were seen in Fig. 5(b) when UV light was switched between ON and OFF states.

In ammonia solutions with different concentrations, the same trend of concentration effect on the open circuit potential was found. When the ammonia concentration was decreased from 0.5% to 0.25%, a slight draft of the potential to a less negative range (ΔE_{min} from −0.31 V to −0.29 V) caused by UV irradiation was found and shown in Fig. 6(a) and (b). For the solutions containing 0.025% ammonia, appreciable change in the voltage was found. The results as shown in Fig. 6(c) indicated that the minimum value of potential (ΔE_{min}) was −0.25 V. This reveals that with the fuel running out gradually, the absolute value of the open circuit voltage of the fuel cell is decreased.

Other types of hazardous materials including Na_2S and ethylene glycol-containing coolant were also used as fuels. Fig. 7(a) and (b) show the open circuit potential (ΔE) vs. time (t) curves obtained from the tests on the solutions containing 0.5 M Na_2S and the coolant with 20% ethylene glycol, respectively. Both Fig. 7(a) and (b) show that when the UV light is ON, the voltage at the photosensitive anode drops to more negative ranges. The 0.5 M Na_2S fuel causes the anode voltage dropping from −0.47 V to −0.58 V when the UV light was switched from OFF to ON. In the coolant, the anode potential was changed from −0.22 V to −0.4 V when the UV light was switched from OFF to ON. Similar to the tests on ammonia and urea solutions, the tests on the photocatalytic decomposition of Na_2S and the coolant can generate electricity. Again, the clean fuel, hydrogen can be produced when the cell was air-tighten or oxygen-free. Due to the limitation to access to hydrogen measurement facility, the hydrogen measurement experiments have not been done.

When Na_2S was put into the fuel cell, the step-by-step oxidation reactions in the solution can be expressed as:

$$S^{2-} + 3OH^- + 6h^+ \rightarrow SO_3{}^{2-} + 3H^+ \tag{9}$$

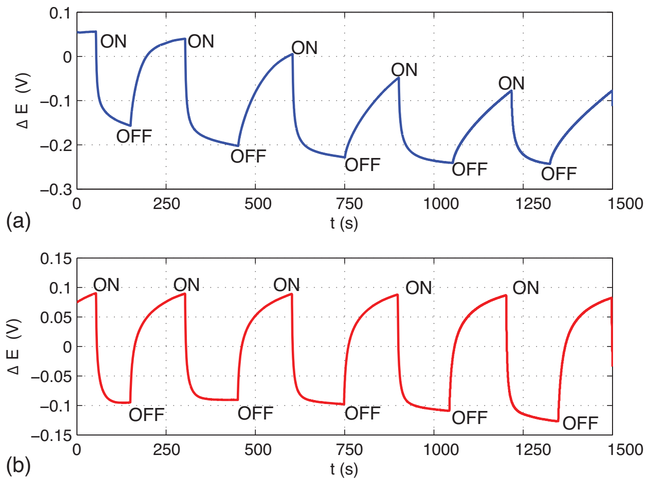

Fig. 5. Effect of concentration on the open circuit voltage of the fuel cell using urea as the fuel: (a) 0.5 M urea solution, (b) 0.25 M urea solution.

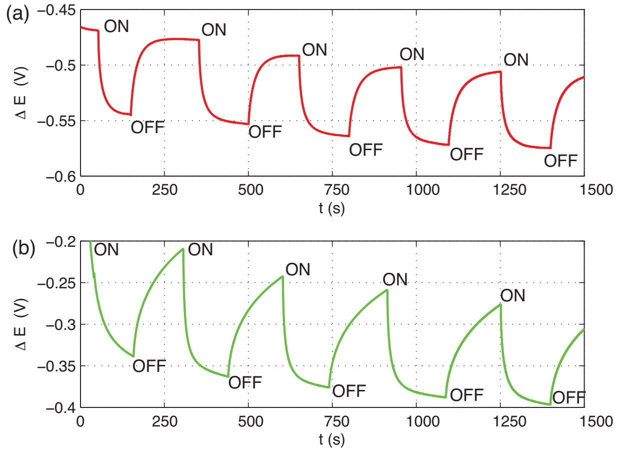

Fig. 7. Open circuit voltage and dynamic response of the photoelectrochemical fuel cell: (a) potential (ΔE) vs. time (t) from the test on the solution containing 0.5 M Na_2S, (b) potential (ΔE) vs. time (t) from the test on the commercial antifreeze/coolant containing 20% ethylene glycol.

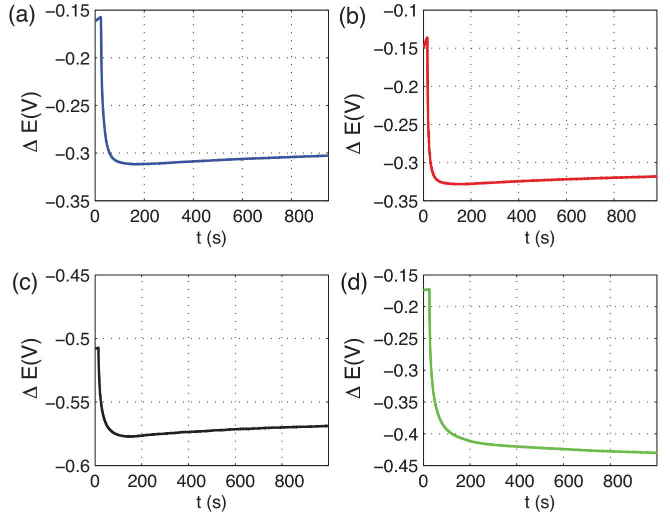

Fig. 8. Time dependent potential change of the photosensitive anode in different solutions under UV illumination: (a) 1.0 M urea, (b) 1% ammonia, (c) 0.5 M Na_2S, (d) the commercial antifreeze/coolant containing 20% ethylene glycol.

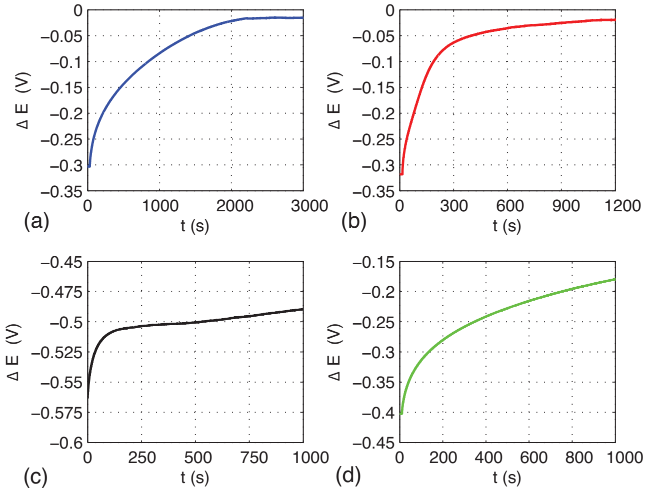

Fig. 10. Time dependent potential recovery of the photosensitive anode in different solutions when the UV light is OFF: (a) 1.0 M urea, (b) 1% ammonia, (c) 0.5 M Na_2S, (d) the commercial antifreeze/coolant containing 20% ethylene glycol.

$$SO_3^{2-} + OH^- + 2h^+ \rightarrow SO_4^{2-} + H^+ \tag{10}$$

At the cathode, clean water generation is the main reaction because the pH value of the 0.5 M Na_2S solution is as high as 13.9. Even under the oxygen-free condition, hydrogen formation is inhibited.

3.4. Photocatalytic reaction kinetics analysis

It is fascinating to examine how fast the decomposition of these waste materials is under the UV light illumination. In Fig. 8, time dependent potential change of the photosensitive anode in different solutions is shown. Fig. 8(a)–(c) show very similar behavior under a considerably long term UV illumination of 1000 s. That is, initially, the potential dropped very rapidly. Then, the potential changed back or was recovered very slowly. This recovery could come from two ways. One is the consumption of the fuels in the three different solutions. Long term exposure to the UV illumination caused the decrease in the fuel concentration. Therefore, the potential shifted back to a more positive range. The extent of this shift can be calculated according to Nernst equation. Another possible reason is the slight increase in the temperature. Since the temperature of the photosensitive anode increases with the absorption of UV light, the mobility of both electrons and holes at the anode and in the fuel increases. The chance for electron–hole charge pair recombination is higher. This recombination leads to the decrease in net charge at the anode. Therefore, the absolute value of the potential is decreased. Consequently, the anode potential shifts to the more positive range. Fig. 8(d) does not show such recovery behavior because the coolant has a much higher concentration of fuel than others. In addition, the coolant has much higher heat conductivity than the other three water based solutions. Therefore, the temperature in the fuel cell can be more uniform. No positive potential shift was observed under such uniform temperature conditions.

In order to analyze the reaction kinetics, the Ti/TiO_2 nanotube-solution half cell and its equivalent circuit are shown in Fig. 9(a) and (b), respectively. In Fig. 9(b), R_1 refers to the photoelectrochemical reaction resistance, while R_2 stands for the resistance of ion transfer in the solutions. Since the circuit is RC type, the exponential change mode of voltage is expected as shown by the curves in Fig. 8. Fig. 9(c) schematically shows the band structure of titanium oxide and the photovoltaic response of the half cell. Under UV illumination, the electron–hole charge pairs are separated. The electrons are ejected into the external circuit, causing the potential shift to more negative values, as shown by the open circuit potential measurements. The holes go into the solutions, contributing to decomposing the existing waste materials.

We also studied the recovery of the photosensitivity induced potential. If the UV light is turned off, the recovery of the potential follows a logarithmic decaying mode as shown in Fig. 10 for the

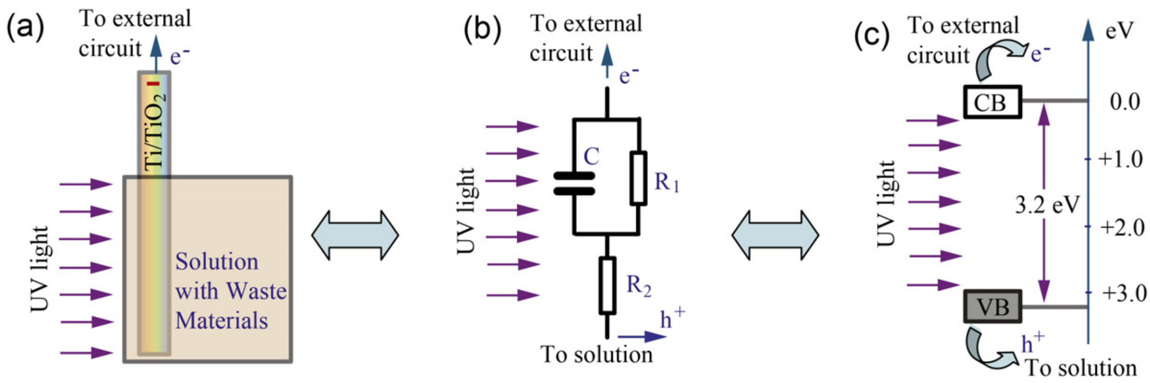

Fig. 9. Illustrations for photocatalytic reaction kinetics analysis: (a) the photosensitive half cell, (b) equivalent circuit simulating the photoelectrochemical reaction, (c) electron–hole charge pair separation at the anode under UV light illumination.

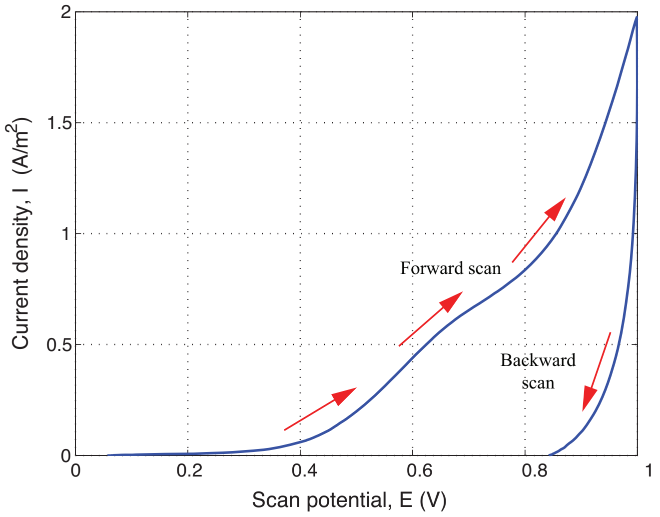

Fig. 11. Current density vs. potential for electroplating Ni on TiO_2 nanotube arrays.

photoelectrochemical fuel cell running on all the four waste materials. This is in agreement with the response of a typical first order model as illustrated in Fig. 9(b). It is deduced that the recovery behavior of the potential is dependent on the electrical and ion conductivity of the solutions. The viscosity of the electrolytes is also taking a role in the potential recovery.

3.5. *Loading TiO_2 nanotubes with nanoparticles to enhance the photocatalytic activity*

Doping has been proven to be an effective way to increase the absorption of titanium oxide material [43–45]. In order to enhance the photocatalytic activity of the TiO_2 nanotube anode, preliminary studies of doping the TiO_2 NTs with a transition metal oxide, NiO, was performed via electroplating Ni to the nanotubes and followed by high temperature annealing at 500 °C for 2 h to convert Ni into NiO. The current–response curve associated with the electroplating is shown in Fig. 11. Ti/TiO_2 was used as the cathode and Pt the anode during the electroplating. Ag/AgCl electrode was used as the reference electrode. The maximum cathode potential scan range is 0–1.0 V. The peak current density is about 2.0 A/m^2 during Ni deposition. The morphology of the NiO nanoparticles was observed by SEM and shown in Fig. 12(a) and (b). Fig. 12(a) shows that the majority of the NiO nanoparticles are deposited inside the nanotubes. In some places, as marked by the arrow at location “A”, there are nanoparticles sticking to the top end of the TiO_2 nanotubes. Fig. 12(b) illustrates the extended NiO materials at the top end of the nanotubes, as marked by the arrow at location “B”. Before converting Ni into NiO, a high resolution transmission electron microscopic (TEM) image was taken using the JEOL 2100F transmission electron microscope. As shown in Fig. 12(c), the sites marked with “Ni” have the dimension of about 8 nm. The TEM images of the regions marked by “Ni” reveal the cubic crystal structure of Ni. To confirm the nanoparticles are nickel, composition analysis was performed using the same TEM. The energy dispersive X-ray diffraction spectrum (EDX) as shown in Fig. 12(d) reveals strong Ni signal. Other elements such as Ti, O, and Cu are also found. Ti and O come from the TiO_2 nanotubes. Cu comes from the edge of the copper grid for holding the TEM sample.

Decomposing hazardous materials using such a doped titanium oxide nanotube anode was conducted using the UV source and a 250 W light bulb. The photosensitivity of the doped anode has been tested under both UV and visible light irradiation and the results are shown in Fig. 13(a) and (b). The preliminary data show that the NiO-doped anode is sensitive to visible light. Form Fig. 13(a), it is found that the UV light causes anode potential to drop −0.15 V. When visible light is used, the change in the potential (about

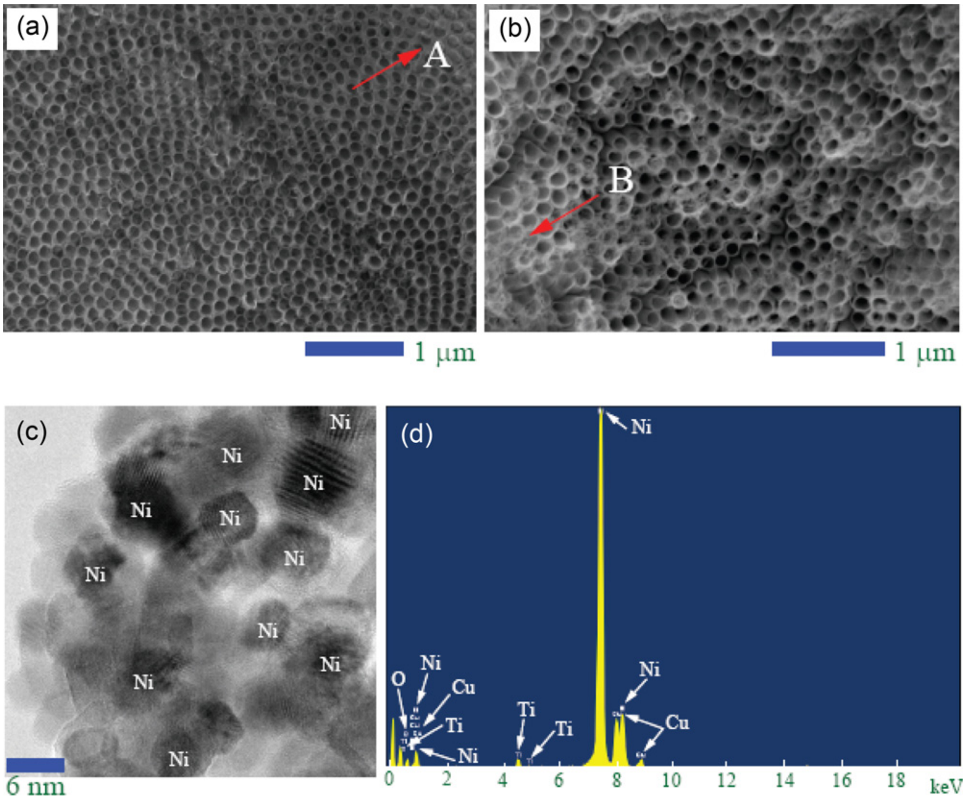

Fig. 12. Electron microscopic analysis showing: (a) NiO particles within and at the top end of TiO_2 nanotubes, (b) NiO particles on the top end of TiO_2 nanotubes, (c) Ni particles with the size of about 8 nm, (d) EDX spectrum.

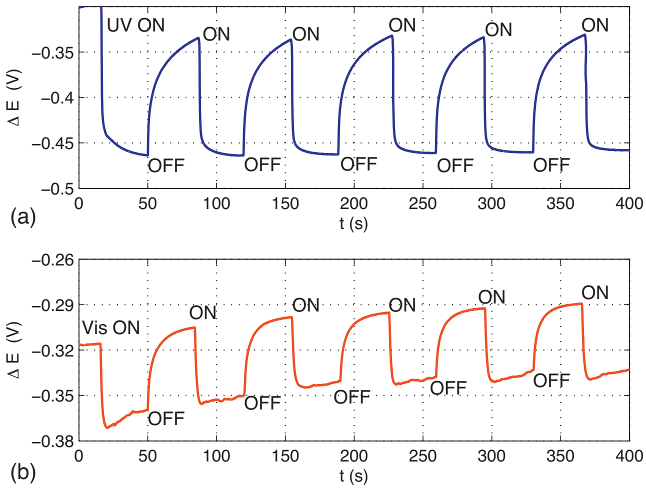

Fig. 13. Effect of NiO doping on the open circuit voltage and dynamic response of the photoelectrochemical fuel cell tested in the solution containing 0.5 M urea: (a) potential (ΔE) vs. time (t) using UV light, (b) potential (ΔE) vs. time (t) using visible light.

−50 mV) as shown in Fig. 13(b) is not as significant as the UV light case. Since pure titanium oxide is not sensitive to the visible light at all, it is concluded that the doped photosensitive anode can harvest photon energy in the visible light spectrum range. The reason for such improvement on the photocatalytic activity is that NiO just like many other oxides [46,47] or sulfide [48,49] can tune the energy gap of the anode, which allows for the doped anode to have visible light absorption capability. It is predicted that the addition of some noble metals such as silver, gold platinum may further enhance the visible light absorption of the nanotubes through the plasmonic effect as found in alumina based nanocomposites [50].

Polyaniline, a conductive polymer, was also deposited to the surface of the photosensitive anode through electrochemical polymerization in a solution containing 0.1 M aniline and 0.5 M sulfuric acid. The CHI400A electrochemical analyzer was used for generating the potential function during the polymerization. The cyclic scan curves are plotted and shown in Fig. 14. The scan voltage range is from −0.2 V to 1.0 V vs. Ag/AgCl reference electrode. The scan rate is 10 mV/s. The current density peak located at 0.42 V as marked by “A” in the plot represents the reaction of polyaniline formation. The first potential scanning cycle only generated a small loop. With the increase of scanning cycles, more and more polyaniline deposited onto the nanotubes and the electrical conductivity of the electrode was increased significantly. Thus, the loop became larger and larger. Totally 20 scan cycles were applied for the polymerization. The loops generated are marked in Fig. 14. The results are useful in analyzing the polymerization kinetics.

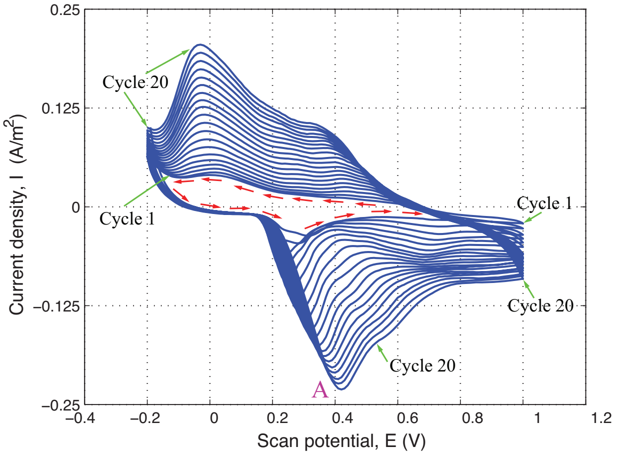

Fig. 14. Current density vs. scan potential associated with electrochemical polymerization of polyaniline on TiO_2 nanotube arrays.

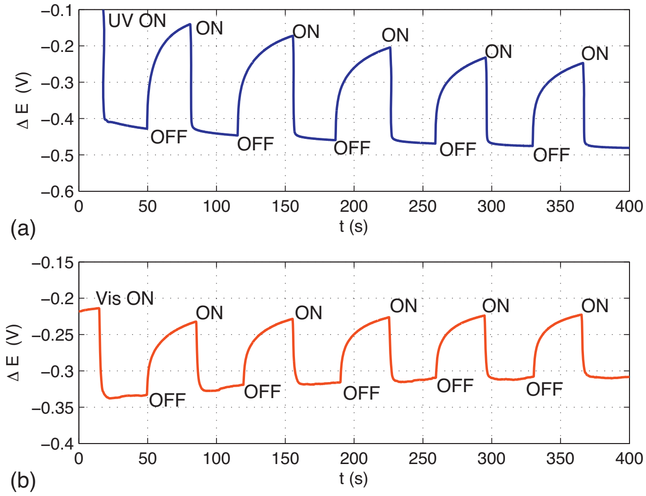

Fig. 15. Effect of polyaniline doping on the open circuit voltage and dynamic response of the photoelectrochemical fuel cell tested in 0.5 M urea solution: (a) potential (ΔE) vs. time (t) using UV light source, (b) potential (ΔE) vs. time (t) using visible light source.

Experiments on the photocatalytic activity show that polyaniline doped TiO_2 NTs have very strong sensitivity to both UV and visible light. Decomposing hazardous materials using such a doped titanium oxide nanotube anode was carried out. The photosensitivity of the doped anode was tested under both UV and visible light irradiation. The test results are shown in Fig. 15(a) and (b). The data reveal that the polyaniline-doped anode is more sensitive to visible light than the NiO-doped anode. Form Fig. 15(a), it can be seen that the UV light causes anode potential to change −0.3 V. When visible light is used, the change in the potential (about −0.11 V) as shown in Fig. 15(b) is very significant even as compared with the UV light case. Obviously, the polyaniline-doped photosensitive anode can harvest photon energy in the visible light spectrum range more efficiently. Since the anode is a multiple component composite materials, it should have a more complex band structure.

The rate of hydrogen formation may be determined by chronocoulometry [51], which is an indirect way to measure the hydrogen amount by the charge consumed at the cathode as long as the main reaction is hydrogen generation at the cathode of the photoelectrochemical fuel cell. The amount of hydrogen generated is related to the charge by Faraday’s law [52]. Each molar of hydrogen corresponds to the 96,500 C electric charge consumed. One molar of hydrogen takes about 22.4 L at the room temperature and at the ambient atmospheric pressure of 1 atm. The volume of the photoelectrochemical fuel cell is about 10 mL. The hydrogen generated per unit volume thus can be determined. Preliminary measurement was done by this method. Systematic work will be performed as our future work.

4. Conclusions

Based on the design, fabrication and characterization of the nanostructured photoelectrochemical fuel cell, the following concluding remarks can be made.

The titanium dioxide nanotubes (TiO_2 NTs) prepared via electrochemical oxidation of pure Ti in an ammonium fluoride and glycerol-containing solution show UV light sensitivity. The oxide nanotubes can be doped with transition metal oxide and conducting polymer materials so that visible light sensitivity can be obtained. Scanning electron microscopic analysis reveals that the nanotubes have an average diameter of 150 nm, wall thickness of 30 nm, and length of 1.5 μm. Such dimensions can be changed by the applied DC voltage level. The higher the voltage is, the thicker the nanotubes.

A novel photoelectrochemical fuel cell with a titanium dioxide nanotube array photosensitive anode has been successfully made. Preliminary data show the feasibility of decomposing environmentally hazardous materials to produce electricity and clean fuel. Although major tests were made by using the UV light source, the visible light sensitivity was also demonstrated. Visible light can be used as the photon energy source upon doping the anode with either the transition metal oxide NiO, or the conducting polymer, polyaniline. The polyaniline-doped photosensitive anode can harvest photon energy in the visible light spectrum range much more efficiently than the NiO-doped nanotubes.

The photosensitive anode made from the highly ordered TiO_2 NTs has the capability of decomposing urea, ammonia, sodium sulfide and automobile engine coolant under ultraviolet (UV) radiation. Also, the anode can decompose these hazardous materials under visible light illumination, but with a lower efficiency. The open circuit potential of the fuel cell is affected by the type and concentration of the waste material solutions.

Acknowledgements

This work was supported in part by The Ohio Board of Regents through the URAF program of University of Toledo. EC was supported by the Undergraduate Research Office, University of Toledo. LS was supported by the Doctoral Instrumentation Graduate Fellowship from College of Engineering, University of Toledo. The transmission electron microscopic (TEM) research carried out at the Center for Functional Nanomaterials, Brookhaven National Laboratory, was supported by the U.S. Department of Energy, Office of Basic Energy Sciences, under contract no. DE-AC02-98CH10886.

References

[1] T.S. Kang, A.P. Smith, B.E. Taylor, M.F. Durstock, Nano Lett. 9 (2009) 601.
[2] Q. Chen, D. Xu, J. Phys. Chem. C 113 (2009) 6310.
[3] K. Shankar, G.K. Mor, H.E. Prakasam, O.K. Varghese, C.A. Grimes, Langmuir 23 (2007) 12445.
[4] Y. Xie, L. Zhou, H. Huang, Appl. Catal. B: Environ. 76 (2007) 15.
[5] K. Shankar, J.I. Bashma, N.K. Allam, O.K. Varghese, G.K. Mor, X. Feng, M. Paulose, J.A. Seabold, K.S. Choi, C.A. Grimes, J. Phys. Chem. C 113 (2009) 6327.
[6] S.K. Mohapatra, M. Misra, V.K. Mahajan, K.S. Raja, J. Phys. Chem. C 111 (2007) 8677.
[7] J.H. Park, S. Kim, A.J. Bard, Nano Lett. 6 (2006) 24.
[8] F.Z. Jia, Z.P. Yao, Z.H. Jiang, C.X. Li, Catal. Commun. 12 (2011) 497.
[9] S. Palmas, A.M. Polcaro, J.R. Ruiz, A. Da Pozzo, M. Mascia, A. Vacca, Int. J. Hydrogen Energy 35 (2011) 6561.
[10] D. Gust, T.A. Moore, A.L. Moore, Acc. Chem. Res. 42 (2009) 1890.
[11] A.J. Bard, J. Phys. Chem. 86 (1982) 172.
[12] N. Getoff, Int. J. Hydrogen Energy 15 (1990) 407.
[13] M. Antoniadou, D.I. Kondarides, D.L. Labous, S. Neophytides, P. Lianos, Sol Energy Mater, Sol. Cells 94 (2010) 592.
[14] D.I. Kondarides, V.M. Daskalaki, A. Patsoura, X.E. Verykios, Catal. Lett. 122 (2008) 26.
[15] M. Li, Y. Li, S. Peng, G. Lu, S. Li, Front. Chem. Chin. 4 (2009) 32.
[16] K.K. Rao, D.O. Hall, Trends Biotechnol. 2 (1984) 124.
[17] L.G. Gassanova, A.I. Netrusov, V.V. Teplyakov, M. Modigell, Desalination 198 (2006) 56.
[18] P.F. Weaver, S. Lien, M. Seibert, Solar Energy 24 (1980) 3.
[19] J.R. Benemann, K. Miyamoto, P.C. Hallenbeck, Enzyme Microbial Technol. 2 (1980) 103.
[20] Y. Miura, Process Biochem. 30 (1995) 1.
[21] G.R. Lambert, G.D. Smith, FEBS Lett. 83 (1977) 159.
[22] M. Modigell, N. Holle, Renew. Energy 14 (1998) 421.
[23] M. Kaneko, H. Ueno, R. Saito, S. Yamaguchi, Y. Fujii, J. Nemoto, Appl. Catal. B: Environ. 91 (2009) 254.
[24] M. Kaneko, H. Ueno, R. Saito, J. Nemoto, Catal. Lett. 131 (2009) 184.
[25] M. Kaneko, H. Ueno, R. Saito, S. Suzuki, J. Nemoto, Y. Fujii, J. Photochem. Photobiol. A: Chem. 205 (2009) 168.
[26] M. Antoniadou, P. Lianos, J. Photochem. Photobiol. A: Chem. 204 (2009) 69.
[27] M. Antoniadou, P. Bouras, N. Strataki, P. Lianos, Int. J. Hydrogen Energy 33 (2008) 5045.
[28] H. Ueno, J. Nemoto, K. Ohnuki, M. Horikawa, M. Hoshino, M. Kaneko, J. Appl. Electrochem. 39 (2009) 1897.
[29] A. Brune, G.J. Jeong, P.A. Liddell, T. Sotomura, T.A. Moore, A.L. Moore, D. Gust, Langmuir 20 (2004) 8366.
[30] K. Suttiponparnit, J.K. Jiang, M. Sahu, S. Suvachittanont, T. Charinpanitkul, P. Biswas, Nanoscale Res. Lett. 6 (2011), http://dx.doi.org/10.1007/s11671-010-9772-1.
[31] V. Kumar, D.H. Adamson, R.K. Prud'homme, Small 6 (2010) 2907.
[32] R. Madhavaram, J. Sander, Y.X. Gan, C.K. Masiulaniec, Mater. Chem. Phys. 118 (2009) 165.
[33] Y.X. Gan, J. Sweetman, J.G. Lawrence, Mater. Lett. 64 (2010) 449.
[34] S.F. Yin, Q.H. Zhang, B.Q. Xu, W.X. Zhu, C.F. Ng, C.T. Au, J. Catal. 224 (2004) 384.
[35] A. Klerke, S.K. Klitgaard, R. Fehrmann, Catal. Lett. 130 (2009) 541.
[36] Y.Y. Hsu, T.L. Hsiung, H.P. Wang, Y. Fukushima, Y.L. Wei, J.E. Chang, Mar. Pollut. Bull. 57 (2008) 873.
[37] J.M. Macak, K. Sirotna1, P. Schmuki, Electrochim. Acta 50 (2005) 3679.
[38] R. Narayanan, T.Y. Kwon, K.H. Kim, Mater. Lett. 63 (2009) 2003.
[39] C.C. Chen, J.S. Lin, E.W. Diau, T.Z. Liu, Appl. Phys. A: Mater. Sci. Proc. 92 (2008) 615.
[40] Z. Zhang, M.F. Hossain, T. Takahashi, Int. J. Hydrogen Energy 35 (2010) 8528.
[41] H. Yang, C. Pan, J. Alloys Compd. 492 (2010) L33.
[42] K. Shankar, G.K. Mor, H.E. Prakasam, S. Yoriya, M. Paulose, O.K. Varghese, C.A. Grimes, Nanotechnology 18 (2007) 065707.
[43] R. Leary, A. Westwood, Carbon 49 (2011) 741.
[44] L. Sun, J. Li, C. Wang, S. Li, Y. Lai, H. Chen, C. Lin, J. Hazard. Mater. 171 (2009) 1045.
[45] M. Miyauchi, A. Nakajima, T. Watanabe, K. Hashimoto, Chem. Mater. 14 (2002) 2812.
[46] M. Fujii, T. Kawai, S. Kawai, Chem. Phys. Lett. 106 (1984) 517.
[47] N. Serpone, P. Maruthamuthu, P. Pichat, E. Pelizzetti, H. Hidaka, J. Photochem. Photobiol. A: Chem. 85 (1995) 247.
[48] P.V. Kamat, N.M. Dimitrijevic, Solar Energy 44 (1990) 83.
[49] V.L. Kuznetsov, P.P. Edwards, ChemSusChem 3 (2010) 44.
[50] Y.X. Gan, X. Zeng, L. Su, L. Yang, B.J. Gan, L. Zhang, Mater. Res. Bull. 46 (2011) 1828.
[51] Y.X. Gan, B.J. Gan, L. Su, Mater. Sci. Eng. B 176 (2011) 1197.
[52] R. Chang, Essential Chemistry, 2nd ed., McGraw-Hill Companies, Inc., Boston, 2000, pp. 628–661.